JOURNAL OF THERMOPHYSICS AND HEAT TRANSFER
Vol. 14, No. 4, October–December 2000

Coupled Radiation and Conduction in a Scattering Composite Layer with Coatings

Ping-Yang Wang,* He-Ping Tan,† and Lin-Hua Liu‡
Harbin Institute of Technology, 150001 Harbin, People's Republic of China
and
Timothy W. Tong§
Colorado State University, Fort Collins, Colorado 80523-1374

Transient coupled radiation and conduction in a two-layer isotropically scattering semitransparent nongray medium with thin opaque coatings is studied by the ray tracing method in combination with Hottel and Sarofim's zonal method (Hottel, H. C., and Sarofim, A. F., *Radiative Transfer*, McGraw–Hill, New York, 1967, pp. 265, 266) and the control-volume method. The radiative energy transfer process in a semitransparent medium is divided into two subprocesses: without considering scattering and considering scattering. The radiative transfer coefficients of the composite are deduced under specular and diffuse reflection, respectively; internal multireflection, total reflection, and refraction are included. The method is extended to gain the radiative transfer coefficients of an isotropically scattering composite with combined specular and diffuse reflection. The radiative heat source term is calculated from the radiative transfer coefficients. The steady-state and transient temperature distributions and heat fluxes in the composite are obtained for the general boundary conditions of external radiation and convection. The present analysis includes the influences of emissivity, surface radiative properties, and spectral properties on the temperature distributions and the heat fluxes.

Nomenclature

A_{k,T_i} = fractional spectral emissive power of spectral band k at nodal temperature T_i: $\int_{\Delta\lambda_k} I_{b,\lambda}(T_i)\,d\lambda \Big/ \int_0^\infty I_{b,\lambda}(T_i)\,d\lambda$
$AI_1, AI_2, \ldots$ = quotient of radiative intensity absorbed by the control volume 2_j; Fig. 3
C_b = unit heat capacity of each layer, $\mathrm{Jm^{-3}\,K^{-1}}$
C_{21} = dimensionless unit heat capacity, C_2/C_1
FT, FA, FJ, FM = functions defined for specular or diffuse reflection; see Eqs. (8), (A5), and (A6)
H_1, H_2 = convection–radiation parameter, $h_1/(\sigma T_r^3)$ and $h_2/(\sigma T_r^3)$, respectively
h_1, h_2 = convective heat transfer coefficient at surfaces of S_1 and S_2, respectively, $\mathrm{Wm^{-2}\,K^{-1}}$
k_{ie}, k_{iw} = harmonic mean thermal conductivity at interfaces, ie and iw, $\mathrm{Wm^{-1}\,K^{-1}}$
L_b = thickness of each layer in the composite, m
L_t = total thickness of composite, $L_1 + L_2$, m
M_b = number of control volumes in each layer
M_t = total number of control volumes in the composite, $M_1 + M_2$
N_b = conduction–radiation parameter, $k_b/(4\sigma T_r^3 L_t)$
NB = total number of spectral bands
n_b = refractive index of the bth layer
n_i = refractive index of the ith control volume; when $i \le M_1 + 1$, n_1, otherwise, n_2
n_s, n_h = smaller and larger refractive index, respectively
P_{refl} = quotient of specular reflection coefficients; Eq. (21)
q^r, q^{cd}, q^{cv} = radiative, conductive, and convective heat fluxes, respectively, $\mathrm{Wm^{-2}}$
$\tilde{q}^r_{S-\infty}, \tilde{q}^r_{S+\infty}$ = dimensionless external radiation fluxes incident at $x = 0$ and L_t; $\sigma T^4_{S-\infty}/(\sigma T_r^4)$ and $\sigma T^4_{S+\infty}/(\sigma T_r^4)$, respectively
$\tilde{q}^t$ = dimensionless total heat flux, $(q^{cd} + q^r)/(\sigma T_r^4)$
S_P = internal interface of two layers; Fig. 1
$(S_bS_c)_k, (S_bV_j)_k, (V_iV_j)_k$ = radiation transfer coefficients of surface vs surface, surface vs volume, and volume vs volume in nonscattering media relative to the spectral band $k(\Delta\lambda_k)$
$[S_bS_c]_k, [S_bV_j]_k, [V_iV_j]_k$ = radiation transfer coefficients of surface vs surface, surface vs volume, and volume vs volume in isotropically scattering media relative to the spectral band $k(\Delta\lambda_k)$
S_1, S_2 = boundary surfaces; Fig. 1
$S_{-\infty}, S_{+\infty}$ = black surfaces denoting the black environment; Fig. 1
T_{g1}, T_{g2} = gas temperatures for convection at $X = 0$ and 1, K; Fig. 1
$\tilde{T}_{g1}, \tilde{T}_{g2}$ = dimensionless gas temperatures, T_{g1}/T_r and T_{g2}/T_r, respectively
T_i = absolute temperature of control volume i, K
T_r = reference temperature or uniform initial temperature, K
T_{S_1}, T_{S_2} = temperatures of the boundary surfaces S_1 and S_2, respectively, K
$\tilde{T}_{S_1}, \tilde{T}_{S_2}$ = dimensionless temperatures, T_{S_1}/T_r and T_{S_2}/T_r, respectively
$T_{S-\infty}, T_{S+\infty}$ = temperatures of the black environment, K, Fig. 1

Received 31 August 1999; revision received 22 May 2000; accepted for publication 25 May 2000.

*Ph.D. Candidate, School of Energy Science and Engineering, 92 West Dazhi Street; wwpy@yahoo.com.
†Professor, School of Energy Science and Engineering, 92 West Dazhi Street.
‡Associate Professor, School of Energy Science and Engineering, 92 West Dazhi Street.
§Professor, Department of Mechanical Engineering. AIAA Associate Fellow.

$TI_1, TI_2, \ldots$	=	fraction of radiative intensity transmitted through an interface; Fig. 3
t	=	physical time, s
t^*	=	dimensionless time $(4\sigma T_r^3 / C_1 L_t)t$
t_s^*	=	steady-state dimensionless time
X	=	x / L_t
x	=	coordinate in direction perpendicular to layer interface, m
$x_{1,1_j}, \ldots$	=	distance of ray transfer between both subscripts, m; Fig. 1
z	=	distance of ray transfer, m
$\alpha_{b,k}$	=	spectral absorption coefficient of layer b, m^{-1}
γ_{bP}	=	transmissivity at internal interface; Fig. 1
Δt	=	time interval, s
Δx	=	spatial interval, m; Fig. 1
δ	=	dimensionless thickness of the first layer, L_1 / L_t
$\varepsilon_{gb}, \varepsilon_{bg}$	=	emissivities at boundary surfaces; Fig. 1
η_i	=	$1 - \omega_i$; when $i \leq M_1 + 1$, ω_1, otherwise, ω_2
Θ	=	dimensionless temperature, T / T_r
θ	=	angle of reflection or incidence
$\kappa_{b,k}$	=	extinction coefficients of layer b, m^{-1}
λ	=	wavelength, μm
μ	=	direction cosine, $\cos(\theta)$
μ_{21}	=	critical direction cosine, $\sqrt{[1 - (n_1/n_2)^2]}(n_1 \leq n_2)$
$\rho_{gb}, \rho_{bg}, \rho_{bP}$	=	reflectivities at interfaces
$\rho_{s\to h}, \rho_{h\to s}$	=	reflectivities, where $s \to h$ is radiation going from a smaller to a larger refractive index and $h \to s$ is from a larger to a smaller refractive index
σ	=	Stefan–Boltzmann constant, Wm^{-2} K^{-4}
$\sigma_{s,k}$	=	spectral scattering coefficient, m^{-1}
$\tau_{b,k}$	=	spectral optical thickness of layer b
Φ_i^r	=	radiative heat source of control volume i
$\omega_{b,k}$	=	spectral single-scattering albedo of layer b, $\sigma_{sb,k}/(\sigma_{sb,k} + \alpha_{b,k})$

Subscripts

a	=	absorbed quotient in the overall attenuated radiative energy
b	=	layer index: 1 in first layer, 2 in second layer; or boundary surface index 1 or 2
bg	=	from layer b to gas
bp	=	from layer b to interface of two layers
c	=	surface index, 1, P, or 2
gb	=	from gas to layer b
h	=	control volume index; see Appendix
i, j, l	=	number of nodes
ie, iw	=	right and left interface of control volume i; Fig. 1
k	=	relative to spectral band k
$1_i, 2_i$	=	ith node in the first layer and the second layer, respectively

Superscripts

d, s	=	diffuse and specular reflection, respectively
$m, m+1$	=	time step
$s + d$	=	combined specular and diffuse reflection

Introduction

WITHIN a semitransparent medium (STM), such as glass,[1,2] ceramics,[3] optical fibers,[4] etc., the temperature and heat flux distributions are affected by radiation in addition to heat conduction. Radiation may be more important when the STM is at elevated temperatures, in high-temperature surroundings, or subjected to large incident radiation.

In the past two decades, some researchers have also focused on the coupled heat transfer in a two-layer or multilayer planar STM in addition to that in a single layer. For example, Tsai and Nixon[5] used the Runge–Kutta method in combination with the finite difference method to study transient coupled radiative and conductive heat transfer in a multilayer semitransparent composite medium under diffuse reflection, in which the boundary surfaces were semitransparent and scattering and internal reflection were ignored. A finite difference method with a variable grid size was used by Timoshenko and Trenev[6] to study the radiative heat transfer in multilayer absorbing–emitting composites, where some of the layers were not in contact and the surfaces were diffuse and semitransparent. By the Galerkin method combined with a finite difference method, Ho and Özisik[7,8] analyzed the transient coupled radiative and conductive heat transfer in a two-layer absorbing, isotropically scattering gray composite medium subjected to external radiation at one of its boundaries. The external boundary surfaces were diffuse and opaque. Siegel[9−11] used the two-flux method in combination with Green's function to study steady-state and transient coupled heat transfer in single layer and multilayer STM with diffuse and semitransparent surfaces. The effects of isotropic scattering, refractive indexes, and spectral properties were considered. Recently, Siegel has reviewed the study of this subject in detail.[12]

In Ref. 13, the transient coupled radiative and conductive heat transfer in an isotropically scattering nongray single-layer STM was investigated by the ray tracing method in combination with Hottel and Sarofim's zonal method[14] and the control-volume method. The radiative properties of various surfaces and thermal boundary conditions are considered. Recently, this method was extended to study the transient coupled heat transfer in an isotropically scattering two-layer STM with the semitransparent boundary surfaces.[15]

The object of this paper is to extend this method to study the transient coupled radiation and conduction in a two-layer isotropically scattering STM with the opaque boundary surfaces. With this aim, the ray tracing method, based on the relations of energy transfer of Hottel and Sarofim's zonal method[14] is used to derive the radiative transfer coefficient (RTC), which is defined as the fraction of the radiative energy absorbed by element j in the transfer process of the radiative energy emitted by element i, of a two-layer isotropically scattering nongray STM with thin coatings at the boundary surfaces. Three reflective characteristics, specular reflection, diffuse reflection, and combined specular and diffuse reflection, are considered. The radiative heat source term is calculated using the RTC and nodal analysis. The transient energy equation is solved by the control-volume method. Spectral properties are considered using the multispectral band model. Comparison of the results in this paper with those of previous work by others shows that the present method without a discrete solid angle is more accurate.

Physical Model and Governing Equations

Physical Model

The analysis is for an absorbing, emitting, and isotropically scattering composite medium composed of a two-layer planar STM with different optical and thermal properties in the different layers. As shown in Fig. 1, the composite medium is between two black surfaces ($S_{-\infty}$ and $S_{+\infty}$), which denote the black environment, whose temperatures are $T_{S_{-\infty}}$ and $T_{S_{+\infty}}$, respectively. Boundary surfaces S_1 and S_2 are opaque, and internal interface S_P is semitransparent. The first layer is divided into M_1 control volumes along its thickness, and the second layer into M_2 control volumes. The ith (or jth) node in the first layer and the second layer are represented by 1_i (or 1_j) and 2_i (or 2_j) respectively. Therefore, $1_i = 1$ (or $1_j = 1$) and $2_i = M_2 + 1$ (or $2_j = M_2 + 1$) represent boundary surfaces S_1 and S_2, respectively. Let $M_t = M_1 + M_2$; then the total number of nodes is $M_t + 2$. For convenience, 1_i (or 1_j) and 2_i (or 2_j) are shortened to i (or j) in the following equations except for the RTC. When i (or j) $\leq M_1 + 1$, i (or j) represents the ith (or jth) node in the first layer and the subscript in the equation is $b = 1$; otherwise, i (or j) represents the $(i - M_1 - 1)$th [or $(j - M_1 - 1)$th] node in the second layer and $b = 2$. Considering transient coupled radiation and conduction, between the time intervals $t (= m\Delta t)$ and $t + \Delta t (= [m + 1]\Delta t)$, the fully implicit discrete energy equation of control volume i is obtained as[15]

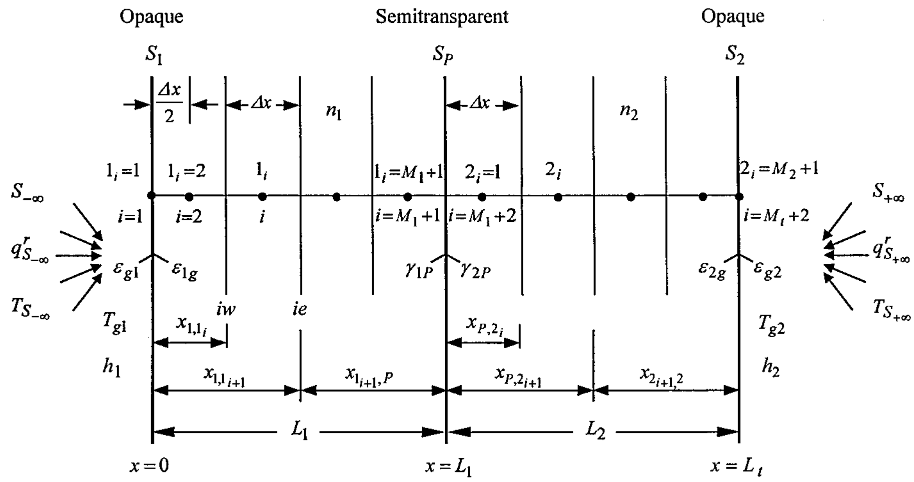

Fig. 1 Zonal discretization model of a two-layer planar composite medium.

$$\frac{C_b \Delta x \left(T_i^{m+1} - T_i^m\right)}{\Delta t} = \frac{k_{ie}^{m+1}\left(T_{i+1}^{m+1} - T_i^{m+1}\right) + k_{iw}^{m+1}\left(T_{i-1}^{m+1} - T_i^{m+1}\right)}{\Delta x} + \Phi_i^{r,m+1}$$

$$2 \le i \le M_t + 1 \qquad (1)$$

Boundary and Initial Conditions

By considering the conditions of coupled surface radiative and convective heat transfer and opaque boundary surfaces, the following boundary conditions are developed.

At surface S_1,

$$q^r_{S_1} + q^{cd} = q^r_{S_1 \to S_{-\infty}} + q^{cv} \qquad (2a)$$

At surface S_2,

$$q^r_{S_2} + q^{cd} = q^r_{S_{+\infty} \to S_2} + q^{cv} \qquad (2b)$$

where $q^r_{S_1 \to S_{-\infty}}$ and $q^r_{S_{+\infty} \to S_2}$ are the radiative heat fluxes between surface S_1 and $S_{-\infty}$ and $S_{+\infty}$ and S_2, respectively. When $i = 1$ and $i = M_t + 2$, the surface radiative heat fluxes $q^r_{S_1}$ and $q^r_{S_2}$ are[16]

$$q^r_{S_1} = \sigma \sum_{k=1}^{NB} \left\{ \left(n^2_{2,k}[S_2S_1]_k A_{k,T_{S_2}} T^4_{S_2} - n^2_{1,k}[S_1S_2]_k A_{k,T_{S_1}} T^4_{S_1} \right) + \sum_{j=2}^{M_t+1} \left(n^2_{j,k}[V_jS_1]_k A_{k,T_j} T^4_j - n^2_{1,k}[S_1V_j]_k A_{k,T_{S_1}} T^4_{S_1} \right) \right\} \qquad (3a)$$

$$q^r_{S_2} = \sigma \sum_{k=1}^{NB} \left\{ \left(n^2_{2,k}[S_2S_1]_k A_{k,T_{S_2}} T^4_{S_2} - n^2_{1,k}[S_1S_2]_k A_{k,T_{S_1}} T^4_{S_1} \right) + \sum_{j=2}^{M_t+1} \left(n^2_{2,k}[S_2V_j]_k A_{k,T_{S_2}} T^4_{S_2} - n^2_{j,k}[V_jS_2]_k A_{k,T_j} T^4_j \right) \right\} \qquad (3b)$$

The discretized forms of Eqs. (2) can be written as

$$q^r_{S_1} + 2k_2 \frac{\left(T_2 - T_{S_1}\right)}{\Delta x} = \sigma \sum_{k=1}^{NB} \varepsilon_{1g,k} \left(A_{k,T_{S_1}} T^4_{S_1} - A_{k,T_{S_{-\infty}}} T^4_{S_{-\infty}} \right) + h_1\left(T_{S_1} - T_{g1}\right) \qquad (x = 0) \qquad (4a)$$

$$q^r_{S_2} + 2k_{M_t+1} \frac{\left(T_{S_2} - T_{M_t+1}\right)}{\Delta x} = \sigma \sum_{k=1}^{NB} \varepsilon_{2g,k} \left(A_{k,T_{S+\infty}} T^4_{S+\infty} - A_{k,T_{S_2}} T^4_{S_2} \right) + h_2(T_{g2} - T_{S_2}) \qquad (x = L_t) \qquad (4b)$$

In Eqs. (4), if convective heat transfer coefficients h_1 and h_2 are infinite, the surface temperature is equal to the environment temperature, that is, $T_{S_1} = T_{g1}$ and $T_{S_2} = T_{g2}$, and Eqs. (4) become first kind boundary conditions. If h_1 is finite but h_2 is infinite, Eqs. (4) become mixed boundary conditions, that is, a first kind boundary condition at surface S_2 and a third kind at surface S_1.

The initial condition for the results given here is a uniform temperature distribution, but the method is valid for an arbitrary initial temperature distribution.

Radiative Heat Source

The key to solving the transient discrete energy equation is to determine the local radiative heat source term Φ^r_i. For a one-dimensional problem, the radiative heat source of control volume i is equal to the difference between the radiative fluxes at its two interfaces[16]:

$$\Phi^r_i = q^r_{ie}(T) - q^r_{iw}(T) = q^r_{ie}(T) - q^r_{(i-1)e}(T), \qquad 2 \le i \le M_t + 1 \qquad (5)$$

When boundary surfaces S_1 and S_2 are opaque, q^r_{ie} can be expressed as

$$q^r_{ie} = \sigma \sum_{k=1}^{NB} \left\{ n^2_{2,k}[S_2S_1]_k A_{k,T_{S_2}} T^4_{S_2} - n^2_{1,k}[S_1S_2]_k A_{k,T_{S_1}} T^4_{S_1} + \sum_{j=2}^{i} \left(n^2_{2,k}[S_2V_j]_k A_{k,T_{S_2}} T^4_{S_2} - n^2_{j,k}[V_jS_2]_k A_{k,T_j} T^4_j \right) + \sum_{j=i+1}^{M_t+1} \sum_{l=2}^{i} \left(n^2_{j,k}[V_jV_l]_k A_{k,T_j} T^4_j - n^2_{l,k}[V_lV_j]_k A_{k,T_l} T^4_l \right) + \sum_{j=i+1}^{M_t+1} \left(n^2_{j,k}[V_jS_1]_k A_{k,T_j} T^4_j - n^2_{1,k}[S_1V_j]_k A_{k,T_{S_1}} T^4_{S_1} \right) \right\} \qquad (6)$$

where when $i, j \le M_1 + 1$, $n_i = n_1$, and $n_j = n_1$, otherwise $n_i = n_2$ and $n_j = n_2$.

From the foregoing deductive process it has been shown that the difficulty in solving for the radiative heat source and the radiative heat flux density is to calculate the RTCs.

RTC of a Composite Layer with Opaque Boundaries

The RTC of a surface or a control-volume element i vs element j is defined as the quotient of the radiative energy absorbed by element j in the transfer process of the radiative energy emitted by element i. For a scattering STM, the transfer process includes 1) the radiative energy directly reaching element j, 2) the reflection by surfaces once or many times, and 3) the scattering by the medium once or many times.

The transfer process of radiative energy can be divided into two subprocesses according to the transfer mechanism in a scattering STM.

1) Only the absorption, emission, and reflection, but not scattering of the medium are considered. For this condition, the RTC are represented by (S_bS_c), (S_bV_j), and (V_iV_j).

2) Only scattering is considered according to the scattering mechanism; for isotropic scattering, the radiative intensity scattered by

element j is distributed uniformly. Such distribution is equivalent to the spatial distribution of the radiative intensity emitted by element j. For this condition, the RTC are represented by $[S_b S_c]$, $[S_b V_j]$, and $[V_i V_j]$.

For convenience, subscript k of the variables denoting spectral properties ρ, γ, ε, ω, and η is omitted in the following processes in the text except for special emphasis.

RTC Without Considering Scattering

RTC for Specular Reflection

In this paper, the energy transfer relations of Hottel and Sarofim's zonal method[14] between surfaces and control volumes, between control volumes and control volumes, and the geometric relations in Fig. 1, as shown in Eqs. (7a–7c), are used to deduce RTC relationships:

$$(S_i V_j) = (S_i S_j) - (S_i S_{j+1}) \qquad (i < j) \tag{7a}$$

$$(V_i V_j) = (S_{i+1} S_j) - (S_i S_j) - (S_{i+1} S_{j+1}) + (S_i S_{j+1}) \qquad (i < j) \tag{7b}$$

$$x_{i,j+1} = x_{i,j} + \Delta x, \qquad x_{i+1,j+1} = x_{i,j}, \qquad x_{i+1,j} = x_{i,j} - \Delta x \tag{7c}$$

Under specular reflection, the incident angle of a ray is equal to the reflective angle. Therefore, the expression for radiative intensity attenuation along the path of a ray emitted at an arbitrary angle can be determined by tracing this ray. Then the RTC considering multiple reflection for an absorbing, emitting STM can be calculated by integrating over a hemisphere in space.

To form a more concise notation, four functions are defined[15]:

$$FT_{b,k}(z) = \exp\left(\frac{-\kappa_{b,k} z}{\mu_b}\right) \tag{8a}$$

$$FJ_{b,k} = \rho_{bP}\rho_{bg} FT_{b,k}(2L_b) \tag{8b}$$

$$FJ_k = \frac{\gamma_{1P}\gamma_{2P}\rho_{1g}\rho_{2g} FT_{1,k}(2L_1) FT_{2,k}(2L_2)}{(1 - FJ_{1,k})(1 - FJ_{2,k})} \tag{8c}$$

$$FA_{b,k} = 1 - FT_{b,k}(\Delta x) \tag{8d}$$

Figure 2 gives the transfer processes of a ray (denotes radiative intensity) in a single-layer STM, in which process 1 denotes the transfer process of the ray coming from surface S_1 and process 2 denotes the transfer process of the ray coming from surface S_2. The radiative intensity fraction reaching surface S_2 in processes 1 and 2 are shown in Ref. 13. The transfer processes of the ray in a two-layer STM with opaque boundary surfaces are given in Fig. 3, in which the beeline with arrowhead within the same layer is equivalent to process 1 of Fig. 2, and the broken line with arrowhead within the same layer is equivalent to process 2 of Fig. 2. The unit radiative intensity of surface diffuse emission finally attenuates to zero due to multiple specular reflection, transmission, and absorption in a single layer. In this process, the total radiative intensities reaching the next surface are[17] for process 1 $FT_{b,k}(L_b)/(1 - FJ_{b,k})$ and for process 2 $FT_{b,k}(2L_b)/(1 - FJ_{b,k})$. In the second layer of Fig. 3, the total radiative intensities reaching control volume 2_j are the beeline with arrowhead, $FT_{2,k}(x_{P,2_j})/(1 - FJ_{2,k})$, and the broken line with arrowhead, $FT_{2,k}(L_2 + x_{2,2_{j+1}})/(1 - FJ_{2,k})$. Referring to Fig. 2 and Fig. 3, the process of determining RTC $(S_1 V_{2_j})_k^s$ is provided here.

As shown in Fig. 3, the radiative intensity emitted toward the STM by surface S_1 at a certain angle finally attenuates to zero due to the processes occurring in the first layer. In these processes, a part of the

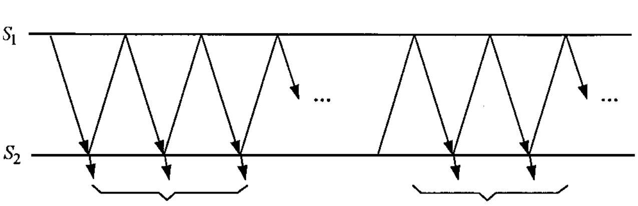

Fig. 2 Radiative intensity propagating in a single-layer STM for specular reflection.

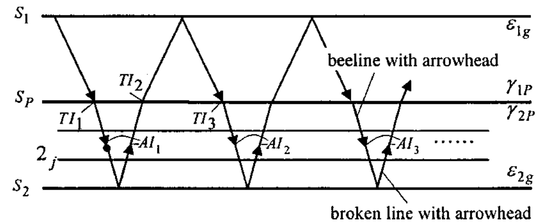

Fig. 3 Radiative intensity propagating in a two-layer STM for specular reflection.

intensity, TI_1, is transmitted into the second layer through interface S_P; the rest is absorbed by surface S_1, and the first layer medium TI_1 can be divided into three parts. The first part, TI_2, comes back to the first layer through interface S_P. The second part, AI_1, is absorbed by control volume 2_j and is called first-order absorption:

$$AI_1 = \varepsilon_{1g}\gamma_{1P}\left(\frac{n_2}{n_1}\right)^2 \times \frac{FT_{1,k}(L_1) FA_{2,k}\left[FT_{2,k}\left(x_{P,2_j}\right) + \rho_{2g} FT_{2,k}\left(L_2 + x_{2,2_{j+1}}\right)\right]}{(1 - FJ_{1,k})(1 - FJ_{2,k})} \tag{9a}$$

The last part is absorbed by surface S_2 and the remaining control volumes of the second layer (except control volume 2_j).

For TI_2, the part denoted by TI_3 is transmitted into the second layer. Just as for TI_1, TI_3 also can be divided into three parts. Thus, the part AI_2 is absorbed by control volume 2_j and is called second-order absorption:

$$AI_2 = \varepsilon_{1g}\gamma_{1P}\left(\frac{n_2}{n_1}\right)^2 \times \frac{FT_{1,k}(L_1) FA_{2,k}\left[FT_{2,k}\left(x_{P,2_j}\right) + \rho_{2g} FT_{2,k}\left(L_2 + x_{2,2_{j+1}}\right)\right](FJ_k)^1}{(1 - FJ_{1,k})(1 - FJ_{2,k})} \tag{9b}$$

By analogy, third-order absorption is

$$AI_3 = \varepsilon_{1g}\gamma_{1P}\left(\frac{n_2}{n_1}\right)^2 \times \frac{FT_{1,k}(L_1) FA_{2,k}\left[FT_{2,k}\left(x_{P,2_j}\right) + \rho_{2g} FT_{2,k}\left(L_2 + x_{2,2_{j+1}}\right)\right](FJ_k)^2}{(1 - FJ_{1,k})(1 - FJ_{2,k})} \tag{9c}$$

and the $(n + 1)$th-order absorption is

$$AI_{n+1} = \varepsilon_{1g}\gamma_{1P}\left(\frac{n_2}{n_1}\right)^2 \times \frac{FT_{1,k}(L_1) FA_{2,k}\left[FT_{2,k}\left(x_{P,2_j}\right) + \rho_{2g} FT_{2,k}\left(L_2 + x_{2,2_{j+1}}\right)\right](FJ_k)^n}{(1 - FJ_{1,k})(1 - FJ_{2,k})} \tag{9d}$$

According to the preceding analysis, in the entire transfer process, in which the radiative intensity emitted by S_1 and comes into the composite medium, then is attenuated to zero. The total radiative intensity absorbed by control volume 2_j is the sum of the geometric progression represented by Eqs. (9). Then RTC $(S_1 V_{2_j})_k^s$ can be calculated by integrating the total radiative intensity over a hemisphere:

$$\begin{aligned}\left(S_1 V_{2_j}\right)_k^s &= 2\int_{\mu_{21}}^{1} [AI_1 + AI_2 + AI_3 + \cdots]\,\mu_2\,\mathrm{d}\mu_2 \\ &= 2\varepsilon_{1g}\gamma_{1P}\left(\frac{n_2}{n_1}\right)^2 \\ &\times \int_{\mu_{21}}^{1} \frac{FT_{1,k}(L_1) FA_{2,k}\left[FT_{2,k}\left(x_{P,2_j}\right) + \rho_{2g} FT_{2,k}\left(L_2 + x_{2,2_{j+1}}\right)\right]}{(1 - FJ_{1,k})(1 - FJ_{2,k})(1 - FJ_k)} \\ &\times \mu_2\,\mathrm{d}\mu_2\end{aligned} \tag{10}$$

For specular reflection, the RTCs of the composite with coatings have the following reciprocal relationships:

$$n_1^2\gamma_{2P}(S_1S_2)_k^s = n_2^2\gamma_{1P}(S_2S_1)_k^s, \qquad \left(S_bV_{b_j}\right)_k^s = \left(V_{b_j}S_b\right)_k^s$$
$$n_1^2\gamma_{2P}\left(S_1V_{2_j}\right)_k^s = n_2^2\gamma_{1P}\left(V_{2_j}S_1\right)_k^s$$
$$n_1^2\gamma_{2P}\left(V_{1_i}V_{2_j}\right)_k^s = n_2^2\gamma_{1P}\left(V_{2_j}V_{1_i}\right)_k^s$$
$$n_2^2\gamma_{1P}\left(S_2V_{1_j}\right)_k^s = n_1^2\gamma_{2P}\left(V_{1_j}S_2\right)_k^s, \qquad \left(V_{b_i}V_{b_j}\right)_k^s = \left(V_{b_j}V_{b_i}\right)_k^s \tag{11}$$

Thus, one of each pair of the RTCs except for $(S_1V_{2_j})_k^s$ is given by Eqs. (12–18):

The RTCs of the opaque surfaces, S_1 and S_2, have no reciprocal relationship and are given next using the form $(S_bS_b)_k^s$

$$(S_bS_b)_k^s = 2\varepsilon_{bg}^2\int_0^1\left\{\frac{\rho_{bP}FT_{b,k}(2L_b)}{(1-FJ_{b,k})} + \frac{\gamma_{bP}\rho_{cg}\gamma_{cP}FT_{b,k}(2L_b)FJ_{c,k}(2L_c)}{(1-FJ_{b,k})^2(1-FJ_{c,k})(1-FJ_k)}\right\}\mu_b\,\mathrm{d}\mu_b \tag{19}$$

where if $b=1$ then $c=2$, otherwise $c=1$; $R_{b,k}=4\kappa_{b,k}\Delta x-2[1-2E_3(\kappa_{b,k}\Delta x)](i=j)$;

$$R_{b,k} = 2\int_0^1 FA_{b,k}^2FT_{b,k}\left(x_{b_i,b_j}\right)\mu_b\,\mathrm{d}\mu_b \qquad (i\neq j)$$

$$(S_1S_2)_k^s = 2\varepsilon_{1g}\varepsilon_{2g}\left(\frac{n_2}{n_1}\right)^2\int_{\mu_{21}}^1\frac{\gamma_{1P}FT_{1,k}(L_1)FT_{2,k}(L_2)}{(1-FJ_{1,k})(1-FJ_{2,k})(1-FJ_k)}\mu_2\,\mathrm{d}\mu_2 \tag{12}$$

$$\left(S_1V_{1_j}\right)_k^s = 2\varepsilon_{1g}\int_0^1 FA_{1,k}\left\{\frac{\left[FT_{1,k}\left(x_{1,1_j}\right)+\rho_{1P}FT_{1,k}\left(L_1+x_{P,1_{j+1}}\right)\right]}{(1-FJ_{1,k})} + \frac{\gamma_{1P}\gamma_{2P}\rho_{2g}FT_{1,k}(L_1)FT_{2,k}(2L_2)\left[FT_{1,k}\left(x_{P,1_{j+1}}\right)+\rho_{1g}FT_{1,k}\left(L_1+x_{1,1_j}\right)\right]}{(1-FJ_{1,k})^2(1-FJ_{2,k})(1-FJ_k)}\right\}\mu_1\,\mathrm{d}\mu_1 \tag{13}$$

$$\left(S_2V_{2_j}\right)_k^s = 2\varepsilon_{2g}\int_0^1 FA_{2,k}\left\{\frac{\left[FT_{2,k}\left(x_{2,2_{j+1}}\right)+\rho_{2P}FT_{2,k}\left(L_2+x_{P,2_j}\right)\right]}{(1-FJ_{2,k})} + \frac{\gamma_{1P}\gamma_{2P}\rho_{1g}FT_{2,k}(L_2)FT_{1,k}(2L_1)\left[FT_{2,k}\left(x_{P,2_j}\right)+\rho_{2g}FT_{2,k}\left(L_2+x_{2,2_{j+1}}\right)\right]}{(1-FJ_{1,k})(1-FJ_{2,k})^2(1-FJ_k)}\right\}\mu_2\,\mathrm{d}\mu_2 \tag{14}$$

$$\left(S_2V_{1_j}\right)_k^s = 2\varepsilon_{2g}\left(\frac{n_1}{n_2}\right)^2\int_0^1 FA_{1,k}\frac{\gamma_{2P}FT_{2,k}(L_2)\left[FT_{1,k}\left(x_{P,1_{j+1}}\right)+\rho_{1g}FT_{1,k}\left(L_1+x_{1,1_j}\right)\right]}{(1-FJ_{1,k})(1-FJ_{2,k})(1-FJ_k)}\mu_1\,\mathrm{d}\mu_1 \tag{15}$$

$$\left(V_{1_i}V_{1_j}\right)_k^s = R_{1,k} + 2\int_0^1\frac{FA_{1,k}^2}{(1-FJ_{1,k})}\left\{\rho_{1g}FT_{1,k}\left(x_{1_i,1}+x_{1,1_j}\right)+\rho_{1g}\rho_{1P}FT_{1,k}\left(x_{1_i,1}+L_1+x_{P,1_{j+1}}\right) + \rho_{1P}FT_{1,k}\left(x_{1_{i+1},P}+x_{P,1_{j+1}}\right)+\rho_{1g}\rho_{1P}FT_{1,k}\left(x_{1_{i+1},P}+L_1+x_{1,1_j}\right) + \frac{\left[\rho_{1g}FT_{1,k}\left(x_{1_i,1}+L_1\right)+FT_{1,k}\left(x_{1_{i+1},P}\right)\right]\left[FT_{1,k}\left(x_{P,1_{j+1}}\right)+\rho_{1g}FT_{1,k}\left(L_1+x_{1,1_j}\right)\right]}{(1-FJ_{1,k})(1-FJ_{2,k})(1-FJ_k)/[\rho_{2g}\gamma_{1P}\gamma_{2P}FT_{2,k}(2L_2)]}\right\}\mu_1\,\mathrm{d}\mu_1 \tag{16}$$

$$\left(V_{2_i}V_{2_j}\right)_k^s = R_{2,k} + 2\int_0^1\frac{FA_{2,k}^2}{(1-FJ_{2,k})}\left\{\rho_{2P}FT_{2,k}\left(x_{2_i,P}+x_{P,2_j}\right)+\rho_{2g}\rho_{2P}FT_{2,k}\left(x_{2_{i+1},2}+L_2+x_{P,2_j}\right) + \rho_{2g}\rho_{2P}FT_{2,k}\left(x_{2_i,P}+L_2+x_{2,2_{j+1}}\right)+\rho_{2g}FT_{1,k}\left(x_{2_{i+1},2}+x_{2,2_{j+1}}\right) + \frac{\left[FT_{2,k}\left(x_{2_i,P}\right)+\rho_{2g}FT_{2,k}\left(x_{2_{i+1},2}+L_2\right)\right]\left[FT_{2,k}\left(x_{P,2_j}\right)+\rho_{2g}FJ_{2,k}\left(L_2+x_{2,2_{j+1}}\right)\right]}{(1-FJ_{1,k})(1-FJ_{2,k})(1-FJ_k)/[\rho_{1g}\gamma_{2P}\gamma_{1P}FT_{1,k}(2L_1)]}\right\}\mu_2\,\mathrm{d}\mu_2 \tag{17}$$

$$\left(V_{1_i}V_{2_j}\right)_k^s = 2\int_{\mu_{21}}^1\frac{\left[\rho_{1g}FT_{1,k}\left(x_{1_i,1}+L_1\right)+FT_{1,k}\left(x_{1_{i+1},P}\right)\right]\left[FT_{2,k}\left(x_{P,2_j}\right)+\rho_{2g}FT_{2,k}\left(L_2+x_{2,2_{j+1}}\right)\right]}{n_1^2(1-FJ_{1,k})(1-FJ_{2,k})(1-FJ_k)\Big/\left[n_2^2\gamma_{1P}FA_{1,k}FA_{2,k}\right]}\mu_2\,\mathrm{d}\mu_2 \tag{18}$$

A limiting condition, $n_1 \le n_2$, is implied in the preceding equations. Thus, the following limiting conditions must be met: if $\mu_2 \le \mu_{21}$, then $\rho_{2P} = 1$.

RTC for Diffuse Reflection

When the RTC is deduced by the ray tracing method for specular reflection, the radiative intensity is determined. For diffuse reflection, the radiative energy is determined, but the tracing process is the same as that for specular reflection, and so it is omitted here. The RTC equations and the reciprocity relationships for diffuse reflection are provided in the Appendix.

RTC for Combined Specular and Diffuse Reflection

In this paper, the RTC equations for combined specular and diffuse reflection are obtained by a linear sum of the RTC equations for specular reflection and that for diffuse reflection:

$$(S_b S_c)_k^{s+d} = P_{\text{refl}} \times (S_b S_c)_k^s + (1 - P_{\text{refl}}) \times (S_b S_c)_k^d \quad (S_b, S_c = S_1, S_2) \tag{20a}$$

$$(S_b V_j)_k^{s+d} = P_{\text{refl}} \times (S_b V_j)_k^s + (1 - P_{\text{refl}}) \times (S_b V_j)_k^d \quad (S_b = S_1, S_2) \tag{20b}$$

$$(V_i S_c)_k^{s+d} = P_{\text{refl}} \times (V_i S_c)_k^s + (1 - P_{\text{refl}}) \times (V_i S_c)_k^d \quad (S_c = S_1, S_2) \tag{20c}$$

$$(V_i V_j)_k^{s+d} = P_{\text{refl}} \times (V_i V_j)_k^s + (1 - P_{\text{refl}}) \times (V_i V_j)_k^d \tag{20d}$$

where P_{refl} is the quotient of specular reflection coefficients:

$$P_{\text{refl}} = \frac{\rho_1^s + \rho_2^s}{\rho_1^s + \rho_1^d + \rho_2^s + \rho_2^d} \tag{21}$$

Determination of Reflectivity

Reflectivity ρ of a semitransparent surface can be obtained from Fresnel's equations (see Ref. 18). When radiation passes into a material of larger refractive index, reflectivity $\rho_{s\to h}$ is

$$\rho_{s\to h} = \int_0^{\pi/2} \left\{ \left[\frac{n_h\cos(\varphi) - n_s\cos(\theta)}{n_h\cos(\varphi) + n_s\cos(\theta)} \right]^2 + \left[\frac{n_s\cos(\varphi) - n_h\cos(\theta)}{n_s\cos(\varphi) + n_h\cos(\theta)} \right]^2 \right\} \sin(\theta)\cos(\theta)\,\mathrm{d}\theta \tag{22a}$$

where θ is the incidence angle, φ is the refractive angle, and $\varphi = \arcsin[n_s \sin(\theta)/n_h]$.

When radiation goes from a larger to a smaller n value, reflectivity $\rho_{h\to s}$ is given by Ref. 19,

$$\rho_{h\to s} = 1 - (n_s/n_h)^2 + \rho_{s\to h}\cdot(n_s/n_h)^2 \tag{22b}$$

where $1 - (n_s/n_h)^2$ is caused by total reflection. For the specular surface, the effect of total reflection is considered in the RTCs. Therefore, $\rho_{h\to s}^s$ becomes

$$\rho_{h\to s}^s = \rho_{s\to h}^s \cdot (n_s/n_h)^2 \tag{22c}$$

For the diffuse surface, although the interfaces are not optically smooth, it is assumed that each bit of roughness acts as a smooth facet[18] and total reflection is considered in the reflectivity so that the reflectivity can be directly obtained from Eqs. (22a) and (22b).

RTC Considering Isotropic Scattering

When the effect of scattering is considered, the fractions of radiative energy represented by RTCs $(S_b S_c)$, $(S_b V_j)$, and $(V_i V_j)$ will be redistributed. For convenience, subscript k and superscripts s, d and $s + d$ are omitted in the following equations. Omission is necessary because, when isotropic scattering is considered, the derivational process and the final form of the RTC equation are the same regardless of whether the medium is spectral or gray and whether there is specular, diffuse, or combined specular and diffuse reflection. The RTC equation for a single-layer absorbing, emitting and isotropically scattering STM is given in Ref. 13.

Taking $[V_i V_j]$ as an example, the derivation of the RTC equation, considering isotropic scattering, is given here. After first-order scattering, for the fraction of energy transfer denoted by RTC $(V_i V_j)$, only η_j is absorbed; that is,

$$[V_i V_j]_a^{1\text{st}} = (V_i V_j)\eta_j \tag{23a}$$

After second-order scattering,

$$[V_i V_j]_a^{2\text{nd}} = [V_i V_j]_a^{1\text{st}} + \sum_{l_2=2}^{M_t+1} \left(V_i V_{l_2}\right)\omega_{l_2}\left(V_{l_2} V_j\right)\eta_j \tag{23b}$$

After third-order scattering,

$$[V_i V_j]_a^{3\text{rd}} = [V_i V_j]_a^{2\text{nd}} + \sum_{l_2=2}^{M_t+1} \left(V_i V_{l_2}\right)\omega_{l_2}\left[\sum_{l_3=2}^{M_t+1}\left(V_{l_2} V_{l_3}\right)\omega_{l_3}\left(V_{l_3} V_j\right)\eta_j\right] \tag{23c}$$

and so on. After the $(n + 1)$th-order scattering, each RTC is given by

$$[V_i V_j]_a^{(n+1)} = [V_i V_j]_a^n + \sum_{l_2=2}^{M_t+1}\left(V_i V_{l_2}\right)\omega_{l_2} \times\left(\sum_{l_3=2}^{M_t+1}\left(V_{l_2}V_{l_3}\right)\omega_{l_3}\left\{\sum_{l_4=2}^{M_t+1}\left(V_{l_3}V_{l_4}\right)\omega_{l_4} \times\cdots\times\left[\sum_{l_{n+1}=2}^{M_t+1}\left(V_{l_n}V_{l_{n+1}}\right)\omega_{l_{n+1}}\left(V_{l_{n+1}}V_j\right)\eta_j\right]\right\}\right) \tag{24a}$$

$$[V_i S_c]_a^{(n+1)} = [V_i S_c]_a^n + \sum_{l_2=2}^{M_t+1}\left(V_i V_{l_2}\right)\omega_{l_2} \times\left(\sum_{l_3=2}^{M_t+1}\left(V_{l_2}V_{l_3}\right)\omega_{l_3}\left\{\sum_{l_4=2}^{M_t+1}\left(V_{l_3}V_{l_4}\right)\omega_{l_4} \times\cdots\times\left[\sum_{l_{n+1}=2}^{M_t+1}\left(V_{l_n}V_{l_{n+1}}\right)\omega_{l_{n+1}}\left(V_{l_{n+1}}S_c\right)\right]\right\}\right) \tag{24b}$$

$$[S_b V_j]_a^{(n+1)} = [S_b V_j]_a^n + \sum_{l_2=2}^{M_t+1}\left(S_b V_{l_2}\right)\omega_{l_2} \times\left(\sum_{l_3=2}^{M_t+1}\left(V_{l_2}V_{l_3}\right)\omega_{l_3}\left\{\sum_{l_4=2}^{M_t+1}\left(V_{l_3}V_{l_4}\right)\omega_{l_4} \times\cdots\times\left[\sum_{l_{n+1}=2}^{M_t+1}\left(V_{l_n}V_{l_{n+1}}\right)\omega_{l_{n+1}}\left(V_{l_{n+1}}V_j\right)\eta_j\right]\right\}\right) \tag{24c}$$

$$[S_b S_c]_a^{(n+1)} = [S_b S_c]_a^n + \sum_{l_2=2}^{M_t+1}\left(S_b V_{l_2}\right)\omega_{l_2} \times\left(\sum_{l_3=2}^{M_t+1}\left(V_{l_2}V_{l_3}\right)\omega_{l_3}\left\{\sum_{l_4=2}^{M_t+1}\left(V_{l_3}V_{l_4}\right)\omega_{l_4} \times\cdots\times\left[\sum_{l_{n+1}=2}^{M_t+1}\left(V_{l_n}V_{l_{n+1}}\right)\omega_{l_{n+1}}\left(V_{l_{n+1}}S_c\right)\right]\right\}\right) \tag{24d}$$

Energy Equilibrium

In the preceding derivation, a basic condition was assumed that the fractions of energy absorbed and scattered must sum to unity.[13]

Because of the integral relationships of the RTC for a nonscattering STM,

$$\sum_{j=1}^{M_t+1} (V_iV_j)_k + (V_iS_1)_k + (V_iS_2)_k = 4\kappa_k V_i \qquad (V_i = \Delta x \times 1 \times 1) \tag{25a}$$

$$(S_bS_1)_k + (S_bS_2)_k + \sum_{j=2}^{M_t+1} (S_bV_j)_k = \varepsilon_{bg,k} \qquad (b = 1 \text{ or } 2) \tag{25b}$$

When calculating the RTC in isotropically scattering media, the RTC for nonscattering media must be normalized first:

$$(V_iV_j)_k^* = (V_iV_j)_k/(4\kappa_k V_i), \qquad (V_iS_c)_k^* = (V_iS_c)_k/(4\kappa_k V_i)$$
$$(S_bV_j)_k^* = (S_bV_j)_k/\varepsilon_{bg,k}, \qquad (S_bS_c)_k^* = (S_bS_c)_k/\varepsilon_{bg,k} \tag{26}$$

where superscript * denotes the normalized value. The inverse operation is performed after the calculation of the $(n+1)$th-order scattering and absorption. Finally, the RTC for isotropic scattering is obtained:

$$[V_iV_j]_k = [V_iV_j]_{a,k}^{(n+1)}\eta_i, \qquad [V_iS_c]_k = [V_iS_c]_{a,k}^{(n+1)}\eta_i$$
$$[S_bV_j]_k = [S_bV_j]_{a,k}^{(n+1)}, \qquad [S_bS_c]_k = [S_bS_c]_{a,k}^{(n+1)} \tag{27}$$

Results and Analysis

Verification of the Computational Method

Comparison of Present Results with Those of Reference 8

To validate the present solution partially, under the assumption that the boundary surfaces of the composite medium are assumed to be covered by thin opaque coatings, the steady-state dimensionless temperatures and heat fluxes here are compared with those in Ref. 8. The input parameters are 1) both of the boundary surfaces are black, $\varepsilon_{1g} = \varepsilon_{2g} = 1$; 2) the boundary conditions are first kind, $\tilde{T}_{S_1} = 0.5$ and $\tilde{T}_{S_2} = 1.0$; and 3) the reflection is ignored at the internal interface; that is, both layers have the same refractive index, $n_1 = n_2 = 1$. Dimensionless heat flux, $\tilde{q}_8^t = q^t/(4n^2\sigma T_r^4)$, is defined by Ref. 8. The results are shown in Table 1. Whether conduction ($N = 1.0$) or radiation ($N = 0.01$) is dominant, the steady-state temperature and net heat flux using the present method are in good agreement with the results of Ho and Özisik.[8] The maximum relative error of temperature is 0.027% and that of net heat flux is 0.061%.

Comparison of Present Results with Those of Reference 20

Machali and Madkour[20] studied radiative heat transfer for combined specular and diffuse reflection in an absorbing and isotropically scattering gray slab. The present method is verified by taking advantage of the case of an isotropically scattering medium (see Table 1 in Ref. 20) with two opaque gray boundaries, in which conduction is neglected. Therefore, $k_1 = k_2 = 1 \times 10^{-12}$ in this paper. Both boundaries are opaque gray surfaces, and boundary temperatures are specified $T_{S_1} = 2T_{S_2}$. The refractive index and the scattering albedo are taken as $n_1 = n_2 = 1$ and $\omega_1 = \omega_2 = 1$. The dimensionless radiative heat flux is defined as follows by Ref. 20:

$$\tilde{q}_{20}^r = |q^r| \big/ \left(2\varepsilon_{1g}\sigma T_{S_1}^r\right) \tag{28}$$

From Table 2, the maximum relative error of the results is 0.015%.

Effect of Emissivities of Opaque Surfaces

For specular reflection, Fig. 4 provides the effect of the emissivity of the external surface at $X = 0$ on steady-state temperature distribution in a gray composite medium for the case $\varepsilon_{1g} = \varepsilon_{2g} = \varepsilon_{g2} = 1$, $\tau_1 = 1$, $\tau_2 = 2$, $\omega_1 = \omega_2 = 0.5$, $\tilde{q}_{S_{-\infty}}^r = 5.0625$, $\tilde{q}_{S_{+\infty}}^r = 1.0$, $N_1 = N_2 = 0.1$, $H_1 = H_2 = 0$, $\delta = 0.5$, $C_{21} = 1$. Here, ε_{g1} is changed from 0 to 0.2 to 1. Each ε_{g1} corresponds to two groups of refractive indexes, $n_1 = n_2 = 1.5$ (solid lines) and $n_1 = 1.5$, $n_2 = 3.0$ (dotted lines). As shown in Fig. 4, with the decrease of ε_{g1}, the temperatures decrease because the energy entering the composite medium from surface S_1 is reduced. When $\varepsilon_{g1} = 0$, that is, surface

Table 1 Comparison of the results in this paper with those in Ref. 8 ($N_1 = N_2 = N$)

				Θ, Ref. 8			Θ, this paper			$\tilde{q}_8^t$	
τ_1	τ_2	ω_1	ω_2	0.25X	0.5X	0.75X	0.25X	0.5X	0.75X	Ref. 8	This paper
						N = 1.0					
2.4	0.6	0	0	0.6402	0.7693	0.8849	0.64030	0.76938	0.88503	0.5947	0.59469
2.4	0.6	0	0.95	0.6393	0.7672	0.8836	0.63939	0.76741	0.88372	0.5910	0.59104
2.4	0.6	0.95	0	0.6321	0.7613	0.8828	0.63215	0.76146	0.88282	0.5821	0.58206
0.6	2.4	0	0	0.6278	0.7519	0.8758	0.62780	0.75186	0.87574	0.5749	0.57491
0.6	2.4	0	0.95	0.6276	0.7517	0.8757	0.62758	0.75170	0.87568	0.5722	0.57221
0.6	2.4	0.95	0	0.6261	0.7518	0.8762	0.62608	0.75181	0.87617	0.5722	0.57225
						N = 0.01					
2.4	0.6	0	0	0.8023	0.9097	0.9409	0.80241	0.90983	0.94084	0.0813	0.08125
2.4	0.6	0	0.95	0.8006	0.9065	0.9469	0.80069	0.90669	0.94705	0.0805	0.08051
2.4	0.6	0.95	0	0.7693	0.9029	0.9427	0.76938	0.90301	0.94265	0.0787	0.07872
0.6	2.4	0	0	0.6957	0.7650	0.8790	0.69546	0.76493	0.87868	0.0786	0.07858
0.6	2.4	0	0.95	0.6937	0.7679	0.8763	0.69364	0.76786	0.87625	0.0774	0.07739
0.6	2.4	0.95	0	0.6489	0.7664	0.8815	0.64875	0.76637	0.88132	0.0772	0.07718

Table 2 Comparison of the dimensionless heat fluxes for slabs

Property	Source	τ_0 = 0.01	τ_0 = 0.1	τ_0 = 0.5	τ_0 = 1	τ_0 = 2	τ_0 = 5
		$\rho_1^d = 0, \rho_1^S + \varepsilon_1 = 1.0, \rho_2^d = 0.2, \rho_2^S = 0, \varepsilon_2 = 0.8$					
ε_1 = 0.2	Ref. 20	0.44559	0.43851	0.41229	0.38554	0.34261	0.25772
P_{refl} = 0.8	This paper	0.445588	0.438534	0.412361	0.385597	0.342634	0.257729
ε_1 = 0.7	Ref. 20	0.39661	0.37798	0.31827	0.26854	0.20591	0.12165
P_{refl} = 0.6	This paper	0.396609	0.377999	0.318315	0.268569	0.205915	0.121657
		$\rho_1^d = 0.2, \rho_1^S = 0, \varepsilon_1 = 0.8, \rho_2^d = 0, \rho_2^S + \varepsilon_2 = 1.0$					
ε_2 = 0.2	Ref. 20	0.11140	0.10963	0.10307	0.09639	0.08565	0.06443
P_{refl} = 0.8	This paper	0.111397	0.109634	0.103090	0.096399	0.085658	0.064432
ε_2 = 0.7	Ref. 20	0.34703	0.33073	0.27848	0.23497	0.18017	0.10645
P_{refl} = 0.6	This paper	0.347033	0.330749	0.278525	0.234998	0.180175	0.106450

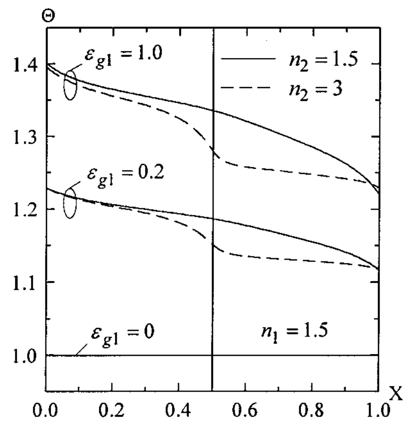

Fig. 4 Effect of outer surface emissivity ε_{g1} on temperature distribution.

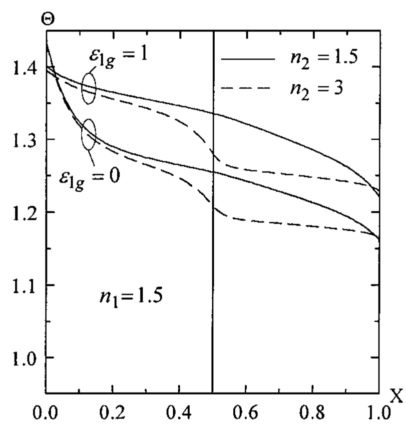

Fig. 5 Effect of inner surface emissivity ε_{1g} on temperature distribution.

S_1 is adiabatic, the temperature distributions become a horizontal line (initial temperature distribution), regardless of whether the refractive indexes of the two layers are the same. When the refractive index of the second layer is changed from 1.5 to 3.0, the temperature gradient in the second layer is decreased.

Figure 5 shows the effect of inner surface emissivity ε_{1g}, at $X = 0$ for specular reflection on the temperature distributions when the parameters are the same as those in Fig. 4, with the exception that $\varepsilon_{1g} = 0$ and 1 and $\varepsilon_{g1} = 1$. As shown in Fig. 5, with an increase in ε_{1g}, the temperatures within the media rise because the energy emitted by surface S_1 increases and the temperatures near surface S_1 somewhat decrease. Compared with Fig. 4, it is seen that the effect of ε_{g1} on temperature distribution is greater than that of ε_{1g}.

Effect of Surface Radiative Properties

When all surfaces of the composite are semitransparent (without coatings), Fig. 6a shows the steady-state temperature distributions for three kinds of reflective characteristics: specular reflection, diffuse reflection, and combined specular and diffuse reflection. Under specular and diffuse reflection, the RTC results for composite media without coatings are provided in Ref. 15, and the RTC results for combined specular and diffuse reflection are calculated using the method in this paper. The input parameters are taken as $n_1 = 1.5$, $n_2 = 3.0$, $\tau_1 = \tau_2 = 0.1$, $\omega_1 = \omega_2 = 0$, $\tilde{q}^r_{S_{-\infty}} = 5.0625$, $\tilde{q}^r_{S_{+\infty}} = 0.0625$, $\tilde{T}_{g1} = \tilde{T}_{g2} = 1.0$, $N_1 = N_2 = 0.025$, $H_1 = H_2 = 5$, $\delta = 0.5$, and $C_{21} = 1$. The reflectivities of the semitransparent interfaces are obtained from Fresnel's equations (see Ref. 18): $\rho_{g1} = 0.0918$, $\rho_{1g} = 0.5964$, $\rho_{1P} = 0.1606$, $\rho_{2P} = 0.7902$, $\rho_{2g} = 0.9196$, and $\rho_{g2} = 0.2762$. For specular reflection, the RTC derived in Ref. 15 considered the effect of total reflection; therefore, the reflectivities can be obtained from Eqs. (22a) and (22c), that is, $\rho_{g1} = 0.0918$, $\rho_{1g} = 0.0408$, $\rho_{1P} = 0.1606$, $\rho_{2P} = 0.0401$, $\rho_{2g} = 0.0307$, and $\rho_{g2} = 0.2762$. For combined specular and diffuse reflection, let $P_{\text{refl}} = 0.6$ (dot–dash lines) and 0.8 (double dot–dash lines). Figure 6b provides the temperature distributions when the parameters are the same as those of Fig. 6a with the exception that $\omega_1 = \omega_2 = 0.9$. It is shown the temperature in the first layer decreases, and the peak value temperature moves to near the interface with an increase in the scattering albedo.

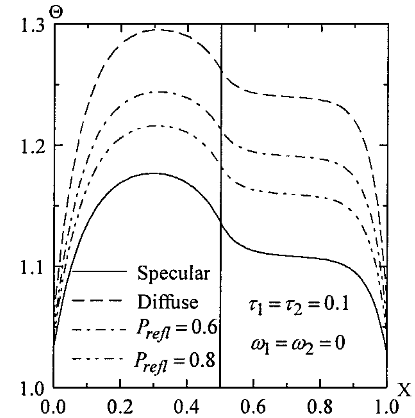

a) Semitransparent boundary surfaces, without considering scattering

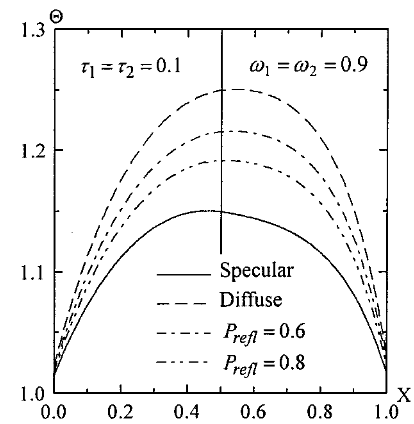

b) Semitransparent boundary surfaces, considering scattering

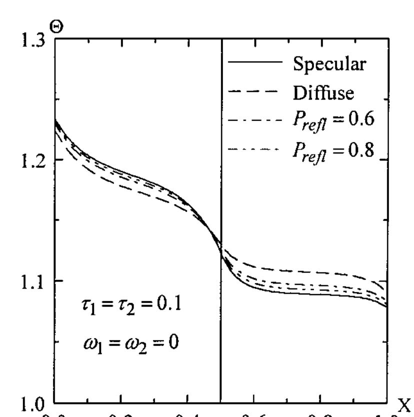

c) Opaque boundary surfaces, without considering scattering

Fig. 6 Effect of surface radiative properties on temperature distribution.

When the external boundaries S_1 and S_2 have a thin opaque coating, for convenience of comparison, the emissivities of the opaque surfaces can be obtained from the reflectivities of the semitransparent surfaces, that is, $\varepsilon_{g1} = 1 - \rho_{g1}$, $\varepsilon_{1g} = 1 - \rho_{1g}$, $\varepsilon_{g2} = 1 - \rho_{g2}$, and $\varepsilon_{2g} = 1 - \rho_{2g}$. The internal interface S_P is still semitransparent. The other parameters are the same as those of Fig. 6a. The results are shown in Fig. 6c.

As shown in Fig. 6a and 6c, when the boundaries are semitransparent, temperature peaks appear within the composite medium. When the boundaries are opaque, the temperature peaks can only appear

Table 3 Dimensionless heat flux $\tilde{q}^t$ for Figs. 6a and 6c

			Combined	
Boundary surface	Specular	Diffuse	P_{refl} = 0.6	P_{refl} = 0.8
Semitransparent	3.42854	2.08666	2.91360	3.17754
Opaque	1.22241	1.38279	1.28959	1.25655

Table 4 Spectral band model for the composite medium

k	λ, μm	$\kappa_{1,k}$, m^{-1}	$\kappa_{2,k}$, m^{-1}	$\omega_{1,k}$	$\omega_{2,k}$
1	0–2	2.0	5.0	0.0	0.0
2	2–5	0.1	0.5	0.0	0.0
3	5–8		Opaque		

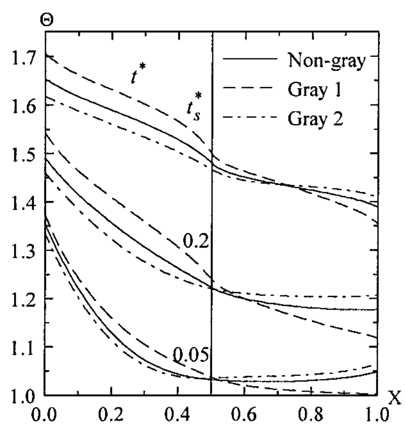

Fig. 7 Effect of spectral properties on transient temperature distribution.

at the heated surface because the radiative energy cannot transfer inside of the medium directly, but can only heat the surface; then energy is transferred inside from the heated surface. The diffuse emission of the opaque surfaces to some extent compensates for the effect of reflective characteristics on the temperature distributions. Thus when the boundary surfaces are opaque, the temperature fields for the three kinds of reflective characteristics are very close. When the boundary surfaces are semitransparent, the effects of the reflective characteristics are more obvious for cases where the optical thickness is smaller and without scattering.

From Figs. 6a–6c, we can see that the temperature fields for combined specular and diffuse reflection fall between those for specular and diffuse reflection. In addition, for all reflective characteristics, the temperature distribution trends are the same when the other parameters are the same. The heat fluxes, when the boundary surfaces are semitransparent, are about double those occurring when the boundary surfaces are opaque. When the boundary surfaces are semitransparent, with a increase in P_{refl} the dimensionless total heat fluxes increase; the trend is inverse when the boundary surfaces are opaque (Table 3).

Effect of Spectral Properties

All of the preceding results are for a gray medium. Now, to illustrate the effect of spectral properties on the transient temperature distributions in a composite medium with coatings, the results under the following three conditions are given in Fig. 7: 1) nongray body, both layers use the same spectral band model (see Table 4); 2) gray body 1, the scattering albedo is kept constant, and the extinction coefficients are $\kappa_{1,k} = 2.0$ and $\kappa_{2,k} = 5.0$ and $\omega_{1,k} = \omega_{2,k} = 0$; 3) gray body 2, the scattering albedo is kept constant, the extinction coefficients are $\kappa_{1,k} = 0.1$ and $\kappa_{2,k} = 0.5$, and $\omega_{1,k} = \omega_{2,k} = 0$. The other parameters are taken as $\varepsilon_{g1} = 0.5$, $\varepsilon_{1g} = \varepsilon_{2g} = \varepsilon_{g2} = 1.0$, $n_1 = 1.5$, $n_2 = 3.0$, $H_1 = 0$, $H_2 = 4$, $N_1 = N_2 = 0.5$, $\tilde{q}^r_{S-\infty} = 8.0$, $\tilde{q}^r_{S+\infty} = 1.0$, $\tilde{T}_{g1} = \tilde{T}_{g2} = 1.0$, $L_1 = L_2 = 1.0$ m, and $C_{21} = 1$. As shown in Fig. 7, 1) the transient temperature fields of the nongray body are between those of both gray bodies and 2) because radiation can provide energy within a material more quickly than diffusion by heat conduction, and the refractive index of the second layer is larger than that of the first layer, the temperature gradient within the first layer for smaller dimensionless time t^* is larger than that for larger t^*. This trend is inverted in the second layer.

Conclusions

A method is developed for studying the transient coupled radiation and conduction in a one-dimensional planar semitransparent nongray composite medium. Under specular or diffuse reflection, the radiative transfer coefficients for a two-layer absorbing and isotropically scattering composite medium with thin opaque coatings are deduced using the ray tracing method and Hottel and Sarofim's zonal method.[14] The present method integrates the solid angle directly. The radiation transfer process can be divided into two subprocesses according to the transfer mechanism of radiative energy in the scattering STM. Thereby, the difficulties of calculating the radiative heat source are reduced. The present method is extended to obtain the RTC values for an isotropically scattering composite for combined specular and diffuse reflection. The radiative heat source term is obtained from the RTC in combination with the nodal analysis, and the transient energy equation is solved by the control-volume method.

Under the conditions of black boundaries and gray media, the temperatures and the heat fluxes in the composite medium are compared with those of Ref. 8. The maximum relative error of temperature is 0.027% and that of net heat flux is 0.061%. For combined specular and diffuse reflection, the heat fluxes in the single layer are compared with those of Ref. 20. The maximum relative error is 0.015%. On this basis, the effects of emissivity, surface radiative properties, and spectral properties of media on the temperature distributions and the heat fluxes are considered. The following conclusions are drawn.

1) The emissivities of the opaque surfaces have great effect on the temperature fields. In addition, the effect of the outer surface emissivity at $X = 0$ is greater than that of the inner surface emissivity at $X = 0$.

2) For cases wherein external heat radiation is incident from one or both sides, temperature peaks may appear within the STM when the boundary surfaces are semitransparent and only at the heated surface when the boundary surfaces are opaque.

3) The temperatures for combined specular and diffuse reflection fall between those for specular and diffuse reflection individually, but the distribution trends are the same.

Appendix: Expressions and Reciprocity Relationships of the RTC Equations for Diffuse Reflection

RTC for an Absorbing, Emitting Composite Medium

Direct RTC

For diffuse reflection, two rays with different launching angles can be mixed. Therefore in this paper, the RTC for diffuse reflection are obtained with tracing the radiative energy using direct radiative transfer coefficient (DRTC). The DRTCs are given as

$$(s_b s_P)_k = 2\int_0^1 \exp\left(\frac{-\kappa_{b,k}L_b}{\mu}\right)\mu\,\mathrm{d}\mu \tag{A1}$$

$$\left(s_c v_{b_j}\right)_k = 2\int_0^1 \left\{\exp\left(\frac{-\kappa_{b,k}x_{c,b_h}}{\mu}\right) - \exp\left[-\kappa_{b,k}\frac{\left(x_{c,b_h}+\Delta x\right)}{\mu}\right]\right\}\mu\,\mathrm{d}\mu \tag{A2}$$

$$\left(v_{b_i} v_{b_j}\right)_k = 2\int_0^1 \left[\exp\left(\frac{-\kappa_{b,k}x_{b_{i+1},b_j}}{\mu}\right) - 2\exp\left(\frac{-\kappa_{b,k}x_{b_i,b_j}}{\mu}\right) + \exp\left(\frac{-\kappa_{b,k}x_{b_i,b_{j+1}}}{\mu}\right)\right]\mu\,\mathrm{d}\mu \qquad (i \neq j) \tag{A3}$$

$$\left(v_{b_i} v_{b_j}\right)_k = 4\kappa_{b,k}\Delta x - 2[1 - 2E_3(\kappa_{b,k}\Delta x)] \qquad (i = j) \quad \text{(A4)}$$

where $b = 1, 2$ and $c = 1, P, 2$; when $b = 1, c = P$ and $b = 2, c = 2$, then $h = j + 1$, otherwise, $h = j$.

For convenience, two functions are defined:

$$FM_{b,k} = \rho_{bP}\rho_{bg}(s_b s_P)_k^2 \quad \text{(A5)}$$

$$FM_k = \frac{\gamma_{1P}\gamma_{2P}\rho_{1g}\rho_{2g}(s_1 s_P)_k^2(s_2 s_P)_k^2}{(1 - FM_{1,k})(1 - FM_{2,k})} \quad \text{(A6)}$$

RTC Equations

The RTC equations are obtained with tracing the radiative energy using DRTC:

$$(S_1 S_2)_k^d = \frac{\varepsilon_{1g}\gamma_{1P}\varepsilon_{2g}(s_1 s_P)_k(s_2 s_P)_k}{(1 - FM_{1,k})(1 - FM_{2,k})(1 - FM_k)} \quad \text{(A7)}$$

$$(S_b S_b)_k^d = \frac{\varepsilon_{bg}^2\rho_{bP}(s_b s_P)_k^2}{1 - FM_{b,k}} + \frac{\varepsilon_{bg}^2\gamma_{bP}\rho_{cg}\gamma_{cP}(s_c s_P)_k^2(s_b s_P)_k^2}{(1 - FM_{b,k})^2(1 - FM_{c,k})(1 - FM_k)} \quad \text{(A8)}$$

$$\left(S_b V_{b_j}\right)_k^d = \frac{\left(s_b v_{b_j}\right)_k + \rho_{bP}(s_b s_P)_k\left(s_P v_{b_j}\right)_k}{FM_{b,k}/\varepsilon_{bg}} + \frac{(s_b s_P)_k(s_c s_P)_k^2\left[\left(s_P v_{b_j}\right)_k + (s_b s_P)_k\rho_{bg}\left(s_b v_{b_j}\right)_k\right]}{(1 - FM_{b,k})^2(1 - FM_{c,k})(1 - FM_k)/[\varepsilon_{bg}\gamma_{bP}\rho_{cg}\gamma_{cP}]} \quad \text{(A9)}$$

$$\left(S_b V_{c_j}\right)_k^d = \frac{\varepsilon_{bg}\gamma_{bP}(s_b s_P)_k\left[\left(s_P v_{c_j}\right)_k + (s_P s_c)_k\rho_{cg}\left(s_c v_{c_j}\right)_k\right]}{(1 - FM_{1,k})(1 - FM_{2,k})(1 - FM_k)} \quad \text{(A10)}$$

$$\left(V_{b_i} V_{b_j}\right)_k^d = \left(v_{b_i} v_{b_j}\right)_k + \frac{\left(s_b v_{b_i}\right)_k\rho_{bg}\left[\left(s_b v_{b_j}\right)_k + (s_b s_P)_k\rho_{bP}\left(s_P v_{b_j}\right)_k\right]}{(1 - FM_{b,k})} + \frac{\left(s_P v_{b_i}\right)_k\rho_{bP}\left[\left(s_P v_{b_j}\right)_k + (s_b s_P)_k\rho_{bg}\left(s_b v_{b_j}\right)_k\right]}{(1 - FM_{b,k})}$$
$$+ \frac{\left[\left(s_b v_{b_i}\right)_k\rho_{bg}(s_b s_P)_k\gamma_{bP} + \left(s_P v_{b_i}\right)_k\gamma_{bP}\right]\rho_{cg}\gamma_{cP}(s_c s_P)_k^2\left[\left(s_P v_{b_j}\right)_k + (s_b s_P)_k\rho_{bg}\left(s_b v_{b_j}\right)_k\right]}{(1 - FM_{b,k})^2(1 - FM_{c,k})(1 - FM_k)} \quad \text{(A11)}$$

$$\left(V_{1_i} V_{2_j}\right)_k^d = \frac{\left[\left(s_1 v_{1_i}\right)_k\rho_{1g}(s_1 s_P)_k\gamma_{1P} + \left(s_P v_{1_i}\right)_k\gamma_{1P}\right]\left[\left(s_P v_{2_j}\right)_k + (s_2 s_P)_k\rho_{2g}\left(s_2 v_{2_j}\right)_k\right]}{(1 - FM_{1,k})(1 - FM_{2,k})(1 - FM_k)} \quad \text{(A12)}$$

In these equations, when $b = 1$, then $c = 2$ and for $b = 2$, then $c = 1$.

Reciprocity Relationships of RTC Equations

For diffuse reflection, the total reflection is considered in the reflectivity and transmissivity, and so the transmissivity and reflectivity of different sides of an interface are different. The reciprocity relationships of RTC equations are given by

$$(S_1 S_2)_k^d\gamma_{2P} = (S_1 S_2)_k^d\gamma_{1P}, \qquad \left(S_b V_{b_j}\right)_k^d = \left(V_{b_j} S_b\right)_k^d$$

$$\left(S_b V_{c_j}\right)_k^d\gamma_{cP} = \left(V_{c_j} S_b\right)_k^d\gamma_{bP}, \qquad \left(V_{1_i} V_{2_j}\right)_k^d\gamma_{2P} = \left(V_{2_j} V_{1_i}\right)_k^d\gamma_{1P}$$

$$\left(V_{b_i} V_{b_j}\right)_k^d = \left(V_{b_j} V_{b_i}\right)_k^d \quad \text{(A13)}$$

where when $b = 1$, then $c = 2$ and when $b = 2$, then $c = 1$.

Acknowledgments

This research is supported by the Chinese National Science Fund for Distinguished Young Scholars, Grant 59725617; the National Natural Science Foundation of China, Grant number 59806003; and Fok Ying Tung Education Foundation, Grant number 71053.

References

[1]Field, R. E., and Viskanta, R., "Measurement and Prediction of the Dynamic Temperature Distributions in Soda Lime Glass Plates," *American Ceramic Society*, Vol. 73, No. 7, 1990, pp. 2047–2053.

[2]Ducharme, R., Kapadia, P., Scarfe, F., and Dowden, J., "A Mathematical Model of Glass Flow and Heat Transfer in a Platinum Downspout," *International Journal of Heat and Mass Transfer*, Vol. 36, No. 7, 1993, pp. 1789–1797.

[3]Thomas, J. R., Jr., "Coupled Radiation/Conduction Heat Transfer in Ceramic Liners for Diesel Engines," *Numerical Heat Transfer, Part A*, Vol. 21, 1992, pp. 109–122.

[4]Yin, Z., and Jaluria, Y., "Zonal Method to Model Radiative Transport in an Optical Fiber Drawing Furnace," *Journal of Heat Transfer*, Vol. 119, 1997, pp. 597–603.

[5]Tsai, C. F., and Nixon, G., "Transient Temperature Distribution of a Multilayer Composite Wall with Effects of Internal Thermal Radiation and Conduction," *Numerical Heat Transfer*, Vol. 10, 1986, pp. 95–101.

[6]Timoshenko, V. P., and Trenev, M. G., "A Method for Evaluating Heat Transfer in Multilayer Semitransparent Materials," *Heat Transfer—Soviet Research*, Vol. 18, 1986, pp. 44–57.

[7]Ho, C. H., and Özisik, M. N., "Combined Conduction and Radiation in a Two-Layer Planar Medium with Flux Boundary Condition," *Numerical Heat Transfer*, Vol. 11, 1987, pp. 321–340.

[8]Ho, C. H., and Özisik, M. N., "Simultaneous Conduction and Radiation in a Two-Layer Planar Medium," *Journal of Thermophysics and Heat Transfer*, Vol. 1, No. 2, 1987, pp. 154–161.

[9]Siegel, R., "Two-Flux Green's Function Analysis for Transient Spectral Radiation in a Composite," *Journal of Thermophysics and Heat Transfer*, Vol. 10, No. 4, 1996, pp. 681–688.

[10]Siegel, R., "Temperature Distribution in a Composite of Opaque and Semitransparent Spectral Layers," *Journal of Thermophysics and Heat Transfer*, Vol. 11, No. 4, 1997, pp. 533–539.

[11]Siegel, R., "Transient Thermal Analysis of Parallel Translucent Layers by Using Green's Functions," *Journal of Thermophysics and Heat Transfer*, Vol. 13, No. 1, 1999, pp. 10–17.

[12]Siegel, R., "Transient Thermal Effects of Radiant Energy in Translucent Materials," *Journal of Heat Transfer*, Vol. 120, 1998, pp. 4–23.

[13]Tan, H. P., Ruan, L. M., Xia, X. L., Yu, Q. Z., and Tong, T. W., "Transient Coupled Radiative and Conductive Heat Transfer in an Absorbing, Emitting and Scattering Medium," *International Journal of Heat and Mass Transfer*, Vol. 42, 1999, pp. 2967–2980.

[14]Hottel, H. C., and Sarofim, A. F., *Radiative Transfer*, McGraw–Hill, New York, 1967, pp. 265, 266.

[15]Tan, H. P., Wang, P. Y., and Xia, X. L., "Transient Coupled Radiation and Conduction in an Absorbing and Scattering Composite Layer," *Journal of Thermophysics and Heat Transfer*, Vol. 14, No. 1, 2000, pp. 77–87.

[16]Tan, H. P., and Lallemand, M., "Transient Radiative—Conductive Heat Transfer in Flat Glasses Submitted to Temperature, Flux and Mixed Boundary Conditions," *International Journal of Heat and Mass Transfer*, Vol. 32, No. 5, 1989, pp. 795–810.

[17]Tan, H. P., Yu, Q. Z., and Lallemand, M., "Transient Combined Radiative–Conductive Heat Transfer at High Temperature in Semi-Transparent Materials," *Chinese Journal of Engineering Thermophysics*, Vol. 10, No. 3, 1989, pp. 295–300.

[18]Siegel, R., and Howell, J. R., *Thermal Radiation Heat Transfer*, 3rd ed., Hemisphere, Washington, DC, 1992, pp. 23, 33, 115.

[19]Richmond, J. C., "Relation of Emittance to Other Optical Properties," *Journal of Research of the National Bureau of Standards Section C: Engineering and Instrumentation*, Vol. 67C, No. 3, 1963, pp. 217–226.

[20]Machali, H. F., and Madkour, M. A., "Radiative Transfer in a Participating Slab with Anisotropic Scattering and General Boundary Conditions," *Journal of Quantitative Spectroscopy and Radiative Transfer*, Vol. 54, No. 5, 1995, pp. 803–813.